MDPI

Article

Modeling the Underwater Sound of Floating Offshore Windfarms in the Central Mediterranean Sea

Marzia Baldachini [1,2,*], Robin D. J. Burns [3], Giuseppa Buscaino [2], Elena Papale [1,2], Roberto Racca [4], Michael A. Wood [3] and Federica Pace [5]

1 Department of Life Sciences and Systems Biology, University of Turin, 10123 Turin, Italy
2 Institute for the Study of Anthropogenic Impacts and Sustainability in the Marine Environment, National Research Council of Italy, 91021 Campobello di Mazara, Italy
3 JASCO Applied Sciences, Droxford SO32 3PW, UK
4 JASCO Applied Sciences, Victoria, BC V8Z 7X8, Canada
5 JASCO Applied Sciences, 24223 Schwentinental, Germany; federica.pace@jasco.com
* Correspondence: marzia.baldachini@unito.it

Abstract: In the shift toward sustainable energy production, offshore wind power has experienced notable expansion. Several projects to install floating offshore wind farms in European waters, ranging from a few to hundreds of turbines, are currently in the planning stage. The underwater operational sound generated by these floating turbines has the potential to affect marine ecosystems, although the extent of this impact remains underexplored. This study models the sound radiated by three planned floating wind farms in the Strait of Sicily (Italy), an area of significant interest for such developments. These wind farms vary in size (from 250 MW to 2800 MW) and environmental characteristics, including bathymetry and seabed substrates. Propagation losses were modeled in one-third-octave bands using JASCO Applied Sciences' Marine Operations Noise Model, which is based on the parabolic equation method, combined with the BELLHOP beam-tracing model. Two sound speed profiles, corresponding to winter and summer, were applied to simulate seasonal variations in sound propagation. Additionally, sound from an offshore supply ship was incorporated with one of these wind farms to simulate maintenance operations. Results indicate that sound from operating wind farms could reach a broadband sound pressure level (L_p) of 100 dB re 1 μPa as far as 67 km from the wind farm. Nevertheless, this sound level is generally lower than the ambient sound in areas with intense shipping traffic. The findings are discussed in relation to local background sound levels and current guidelines and regulations. The implications for environmental management include the need for comprehensive monitoring and mitigation strategies to protect marine ecosystems from potential acoustic disturbances.

Keywords: anthropogenic noise; Strait of Sicily; floating offshore turbines; sound propagation; marine pollution

1. Introduction

Offshore wind power is gaining importance in the transition toward more sustainable energy production, witnessing significant growth in recent years [1]. However, this expansion raises concerns regarding the potential environmental impacts that remain poorly studied [2–6].

The development of offshore wind farms could contribute to localized noise during the construction, operation, and maintenance phases [4,7]. Construction activities and turbine operation generate underwater sound that can disrupt vital behaviors, such as communication, navigation, and feeding patterns, potentially leading to physiological stress, habitat displacement, and altered community dynamics within affected marine ecosystems. The impacts of anthropogenic sound have been described in several species of both vertebrates and invertebrates [8–11], raising concerns for biodiversity conservation. Indeed, regulations

have begun to consider underwater noise as an indicator of marine environmental quality. The European Marine Strategy Framework Directive [12] includes underwater noise as a descriptor (D11) for good environmental status (GES) mandating member states evaluate and track its levels. The descriptor D11C2 [13] focuses on continuous noise in the 63 Hz and 125 Hz one-third-octave bands. Sound from operational wind turbines could be considered continuous, and its monitoring would fall under this descriptor.

Recent studies and gray literature reports [14–17] evaluated the operational underwater sound generated by wind turbine generators (WTGs), focusing on fixed-bottom foundations.

Floating foundations are a relatively new technology, with only a few wind farms having been installed at full scale. In contrast to fixed foundations, these are buoyant structures that are anchored to the seabed through mooring lines. The following four types of floating foundations are known: a simple spar buoy, a semi-submersible, a tension-leg system, and a barge [18]. Currently, the few installed full-scale floating wind farms use either spar or semi-submersible platforms [19], which are the most advanced and tested technologies so far. The tension-leg system and barge platforms remain largely in the experimental or conceptual stages, with no full-scale installations reported to date. The mooring lines connect the floating structure to the seabed; they vary according to the (a) type of floater and (b) type of seabed, which determine the anchor required, varying from suction buckets to piles or drag anchors. Spar buoys are typically held in place by catenaries, while semi-submersibles may be fixed using tension legs or catenaries. Different mooring systems are subject to different types and extents of motion and therefore will vibrate differently in response to the surrounding media.

Sound from operational wind turbine generators can originate from several potential sources, such as the blade rotation and vibrations within the nacelle [15]. These vibrations are caused by both the mechanical elements and wind force, propagating through the turbine tower to the foundation, and radiating underwater sound energy, mostly under 1 kHz with distinct tones matching the gear rotation and harmonics [15]. In turbines equipped with a gearbox system, radiated sound can also be influenced by the gear ratio and generator operation rates [20–22]. Furthermore, an increase in blade size leads to higher mechanical forces on gears and bearings, causing increased sound levels, which also happens with higher wind speeds [16]. These mechanically induced sounds are generated in any type of WTG, independently of whether they are fixed or floating foundations, although their coupling to the water medium is dependent on the extent and shape of the submerged section of the structure. An additional source of underwater sound for floating WTGs is their mooring systems [23]. The sound emissions generated by the moorings are still poorly known because only a few floating wind farms have been constructed, and it is unclear whether their sound emissions have been monitored.

Since floating WTGs are still an infrequently deployed technology, their underwater sound contribution has only recently begun to be studied in detail [23,24]. The only two OWFs monitored until now have been Hywind Scotland [23] and Kincardine [24], reporting median operational broadband source levels up to 167.2 dB re 1 $\mu Pa^2 m^2$ with 15 knots wind speed at Hywind Scotland [23] and 148.8 dB re 1 μPa at Kincardine [24]. These two OWFs have the following different flotation devices: a spar buoy (elongated, vertically oriented float with round cross-section) and a semi-submersible platform with three vertical cylindrical floats, respectively [19]. The latter system, developed by Principle Power and known as WindFloat®, is ballasted by transferring water in or out of the cylinders through internal pumps to enhance stability. These pumps represent an ulterior potential source of sound emissions transmitted underwater. The use of the pumps is of short duration, as they are activated when changes in weather conditions occur. While, in principle, these pumps function similarly to the ballasting pumps of ships, their underwater sound signature is still poorly understood.

For either the spar or the semi-submersible foundation types, most turbine operational noise is concentrated below 200 Hz [24]. Semi-submersible turbines show distinct tonal features between 50 and 80 Hz [24], while dominant tones from spar foundation turbines

were observed at about 25 and 75 Hz [25]. Semi-submersible platforms appear to cause a higher occurrence of impulsive "snaps" or transients from mooring-associated structures when wind speed increases [24]. The sound of the moorings is associated with a 100–400 Hz frequency range. The primary environmental factor affecting movement and the friction of mooring components in the floating structure is wave height [23].

Operational sound from offshore wind farms was at first not deemed environmentally concerning because sound levels were significantly lower compared to the construction phase [26], but the trend toward larger, higher-power installations necessitates a focus on the impact of aggregate sound from multiple turbines, especially in relation to the already existing noise pollution. Maintenance operations throughout the lifespan of offshore wind farms can also introduce the following additional sources of continuous noise: support ships employed for maintenance at large wind farms could stay in the area for multiple days and, by keeping dynamic positioning (i.e., the vessel automatically maintains its heading and position thanks to a computer-controlled system and without the use of mooring lines or anchors), introduce considerable low-frequency sound [10].

Acoustic propagation models are critical tools in underwater acoustics, providing a framework to predict how sound travels through the marine environment [27–29]. These models are widely used for predicting the possible impact of anthropogenic noise on marine ecosystems [23,26,30]. However, the effects of different seasons on sound propagation have not been examined. Variations in sound speed profiles, influenced by water temperature, salinity, and pressure, result in complex spatial and temporal changes in sound propagation [29]. Including diverse sound speed profiles enables more accurate modeling of acoustic phenomena, contributing to the improved understanding and management of underwater environments.

Currently, there are over 130 offshore wind farm projects being planned in Italian waters [31]. These projects are primarily located offshore of the regions of Apulia, Sicily, and Sardinia, which are considered strategic areas for the installation of wind farms due to their favorable environmental conditions and the availability of adequate maritime space. The Strait of Sicily, a hotspot of biodiversity in the Central Mediterranean Sea [32,33], is one of the areas most involved in Italian offshore wind farm development plans, with more than ten projects at different planning stages [31]. This marine area is strongly affected by vessel traffic [34], as it hosts some of the main shipping lanes of the Mediterranean, as well as intense fishing activities, contributing to continuous low-frequency noise. Furthermore, smaller motorized vessels add intermittent noise across a higher range of frequencies [35]. The strait was identified as a noise hotspot for shipping noise by the Agreement on the Conservation of Cetaceans of the Black Sea, Mediterranean Sea and Contiguous Atlantic Area (ACCOBAMS) and one of the few that overlaps with important cetacean habitats [36].

Given the high number of projects planned in the Strait of Sicily and the biological importance of the area, this study aims to predict the potential impacts of the operation of multiple wind farms within that body of water. Since this potential radiated sound cannot be evaluated by examining only single turbine propagated levels [16], we modeled the aggregate sound generated by all turbines. Three wind farm projects in the Strait of Sicily were considered for propagation modeling. The objectives of this study include (1) describing the potential propagated sound of the three offshore wind farms considering broadband levels; (2) describing the potential propagated sound at the dominant frequencies' one-third-octave bands, as well as 63 Hz and 125 Hz one-third-octave bands mandated by the MSFD; (3) evaluating possible variations in the sound distribution in relation to the seasonal conditions; (4) comparing the sound radiated by the three wind farms based on the area's characteristics (bathymetry, sediment features, and sound speed profile); and (5) examining the possible acoustic contribution of a maintenance ship to an operating wind farm.

The results offer an acoustic description of operational offshore wind farms, considering the specific environmental characteristics, and simulating the presence of an offshore

supply ship in dynamic positioning for maintenance operations. The findings might enhance confidence in future assessments of potential impacts on the marine ecosystem.

2. Materials and Methods

2.1. Offshore Wind Farm Project Descriptions

Three wind farms were chosen for the acoustic propagation modeling of operational sound. Hannibal (Northwestern Sicily Strait, 7SeasMed), Sicily South (north-central Sicily Strait, AvenHexicon), and Med Wind (Southern Tyrrhenian Sea—northern Sicily Strait, Renexia) represent a variety of wind farm sizes and bathymetries (Table 1). Since Med Wind is the farthest wind farm from shore, covering the widest area and accounting for a large number of turbines, an offshore support ship will possibly be used for maintenance operations, staying at the farm for several hours or days. Therefore, we also added its acoustic contribution to the aggregate sound (acoustic footprint) of the wind farm.

Table 1. Offshore wind farm (OWF) names, sizes, power of single turbines and total wind farm, and depth range in the area [37–40].

OWF Name	Proposed Number of Turbines	Single Turbine Power (MW)	Total Power (MW)	Depth Range (m)
Hannibal	21	12	250	200–350
Sicily South	48	25	1200	290–525
Med Wind	190	14.7	2800	100–900

The Hannibal floating offshore wind farm is scheduled for construction approximately 37 km from the shores of Marsala and 32 km from Marettimo Island (Egadi Islands, Strait of Sicily). This project will comprise 21 floating turbines, each with a nominal power of 12 MW, resulting in a total capacity of 250 MW [37] (Table 1). The Sicily South wind farm is set to be established within the central area of the Strait of Sicily. This project will feature 24 triangular-shaped floating foundations, each accommodating two turbines with a nominal power of 25 MW. The combined capacity of this installation should reach 1200 MW [38] (Table 1). The Med Wind floating wind farm is planned for development off the coast of the Egadi Islands, situated between the Southern Tyrrhenian Sea and the Strait of Sicily. This project will include 190 wind turbines grouped into three subfields (A1: 62 turbines, A2: 62 turbines, A3: 66 turbines). With a nominal power of 14.7 MW per turbine, the entire installation is expected to generate approximately 2800 MW of power [39] (Table 1).

2.2. Wind Farm Turbine Layouts and Bathymetry

Turbine layouts were extracted from the most up-to-date reports published on the Ministry of the Environment and Energy Security website [37–39]. They were georeferenced with QGIS v. 3.28.6, and for each wind farm, a point vector layer was created to locate the georeferenced turbines (Figure 1). The most accurate coordinates of all turbines were extracted in Easting and Northing format according to the WGS 84/UTM Zone 33 Coordinate Reference System (EPSG:32633). Bathymetry grids were downloaded from GEBCO (2023) [40] and imported into QGIS as raster layers to extract the depth of each turbine location. Sediment data for the areas were taken from the seabed substrate map on the European Marine Observation and Data Network (EMODNet) (multiscale folk 7) [41].
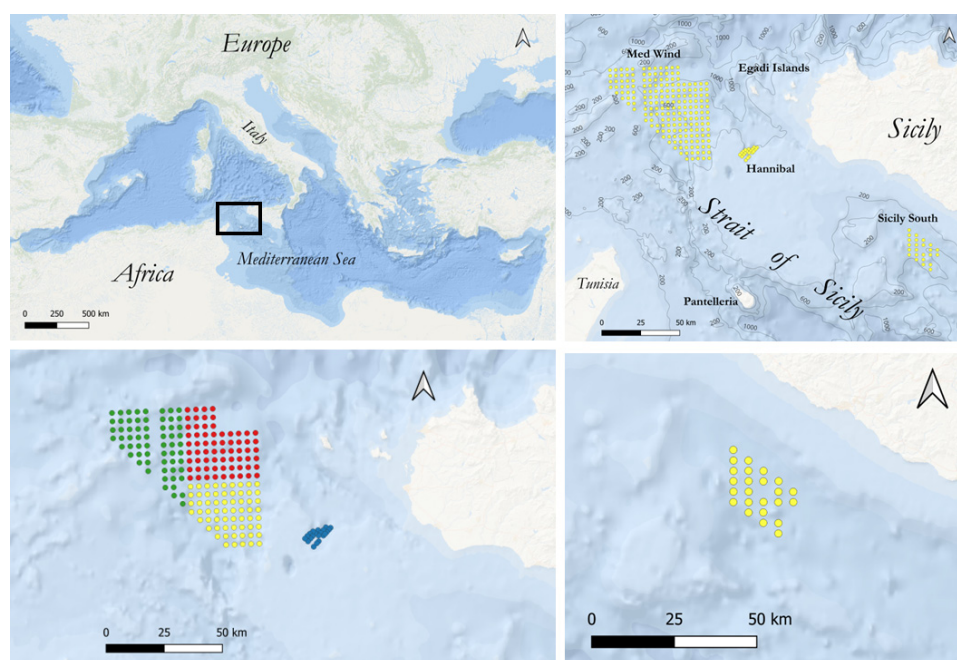
Figure 1. In the top left image, featuring the Mediterranean basin, highlighting the map part that is enlarged in the image on the top right, are all modeled wind farms, with each yellow dot representing a turbine. On the bottom left is the layout of Med Wind, with 190 turbines (A1 in green; A2 in yellow; A3 in red), and Hannibal, with 21 turbines. On the bottom right is the layout of Sicily South, with 48 turbines on 24 foundations.

2.3. Source Modeling

Since this study is focused on the aggregate far-field sound levels from multiple turbines, the sound propagation modeling assumes that a turbine can be represented as a point source. The local features of near-field contributions from individual sources have been considered irrelevant. Furthermore, there is no anticipated strong directivity pattern in the sound emissions that would necessitate a more complex modeling.

Two source locations were chosen for each wind farm or subsite to represent different bathymetries. These locations were used as proxies for all the other source locations to account for the total number of turbines based on similarity in bathymetry (Table 2).

Table 2. Modeling source locations, depths, coordinates (WGS 84/UTM zone 33N–EPSG:32633), and abbreviations for each wind farm or subsite.

OWF Name	Location Depth (m)	Easting (m)	Northing (m)	Abbreviation
Hannibal	Deepest, 340	239,241	4,167,500	HB-D
Hannibal	Median, 224	237,158	4,165,152	HB-M
Sicily South	Deepest, 627	354,985	4,100,305	SS-D
Sicily South	Median, 511	341,781	4,112,948	SS-M
Med Wind A1	Deepest, 806	179,913	4,211,809	A1-D
Med Wind A1	Shallowest, 213	172,825	4,222,559	A1-S
Med Wind A2	Deepest, 692	201,305	4,186,623	A2-D
Med Wind A2	Median, 492	208,308	4,175,845	A2-M
Med Wind A3	Deepest, 884	194,156	4,222,623	A3-D
Med Wind A3	Median, 516	211,882	4,201,031	A3-M

For Hannibal, Sicily South, and the Med Wind subsites A2 and A3, the deepest water location was used as a representative source position to model all turbine sites with a water depth greater than the median, and the median water depth location was used to model all sites with a water depth shallower than the median. In the sole case of Med Wind A1,

the shallowest water location, rather than the median, was used as a representative source position to model all turbine sites with a water depth shallower than the median.

The source was modeled approximately at the midpoint (10 m depth) of the submerged part of a hypothetical semi-submersible foundation [42] since this is the foundation type that could be used for the considered wind farms. This source location accounts for the underwater sound emission from the vibration of rotating machinery within the aerogenerator, as well as mechanical structures below the water line, yielding a representative simplification of sound propagation from the overall assembly. Source levels are taken from the backpropagated measurements for the Hywind Scotland offshore wind farm, as described below. In that study, the sound was backpropagated to the midpoint of the submerged section to determine the source levels using the same sound propagation model used here. This justifies using a point source at the mid-depth of the submerged structure as an appropriate method for repropagating the sound.

Since only a few spectra are available in the literature, the median one-third-octave band sound levels of Hywind Scotland spar-type floating turbines operating at different wind speeds were applied. Through backpropagation modeling, spectra were calculated at 10 knots and 15 knots of wind speed [23,25] and are reported in the Supplementary Materials (Table S1).

Wind speed grids in the Strait of Sicily were downloaded from Copernicus Marine Service [43] and imported into QGIS as raster layers. Wind speed data at all source locations were sampled from these raster layers. To exemplify contrasting seasons, the median wind speeds during February 2023 and August 2023 were considered for each source location; they are reported in the Supplementary Materials (Table S2) together with the closest wind speed values at which the Hywind spectra were calculated.

2.4. Propagation Loss Modeling

Propagation losses were modeled in one-third-octave bands using the Marine Operations Noise Model (MONM, JASCO Applied Sciences) [44] based on the parabolic equation method for frequency bands from 10 to 800 Hz [45], combined with a beam-tracing model [46] from 1 to 25 kHz. MONM is proprietary software belonging to JASCO; it is, however, largely based on publicly available code (RAM [45] for parabolic equation and BELLHOP [46] for ray tracing). The predictions from MONM have been validated against experimental data from numerous underwater acoustic measurement programs conducted by JASCO [47–55].

The bathymetry information used for propagation modeling was obtained from EMODnet [41] and gridded onto a cartesian grid with a resolution of 250 m. Temperature and salinity profiles, from which the sound speed profiles were computed, were extracted from the US Naval Oceanographic Office's Generalized Digital Environmental Model V 3.0 [56,57] for the months of February and August to have a representation of the changes in the acoustic propagation during seasons (Supplementary Materials, Figure S1). Geoacoustic profiles were generated using the sediment information from EMODnet [41] and the sediment parameters by Hamilton [58]. All geoacoustic profiles are reported in the Supplementary Materials (Hannibal: Tables S3 and S4; Sicily South: Tables S5 and S6; Med Wind: Tables S7–S12).

The turbine source levels were determined through backpropagation using MONM with BELLHOP [25]; consequently, using the same models for repropagation is the most robust method for sound level predictions. Sound propagation loss was modeled at the center frequency for each band in radial transects from the source location with an angular resolution of 2.5° to a maximum distance of 100 km. At higher frequencies, at which propagation is more limited by absorption and reflective losses, the maximum distance was determined by considering the distance at which energy in this frequency band did not contribute to the overall broadband level. The range resolution of the output was 20 m, with receiver depths on a variable grid covering the entire water column.

The propagation losses were applied to the operational turbine source levels to determine received sound levels as a function of frequency, depth, and distance from the turbine. These were interpolated onto cartesian grids to provide received level output grids for each modeled source location. To model the aggregate sound of the wind farms, the appropriate single-turbine output grids were recentered (transposed) on each turbine location for each wind farm, as explained in Section 2.3. Both broadband levels and one-third-octave band levels at 63 Hz, 100 Hz, 125 Hz, and 200 Hz center frequencies were estimated. Results are expressed in both sound levels (L_p) (see Results) and sound exposure levels over 24 h (Supplementary Materials, Table S13).

2.5. Offshore Supply Ship Sound Modeling

The motor vessel Siem Sapphire was chosen as an example of an offshore supply ship that could be reasonably used for maintenance at a large wind farm far from the coast such as Med Wind. It is 91 m long with a draught of 7 m [59]. Siem Sapphire's sound levels were recorded [59] during dynamic positioning. Propagation losses in the Otway Basin environment were modeled to backpropagate the vessel's measured levels to the source and generate a spectrum of source levels that is independent of the acoustic environment [59].

Propagation losses in the Med Wind area were modeled using the method described in Section 2.4. The modeling assumed that a point source can represent a vessel in dynamic positioning. The source depth for modeling ship sound propagation is set at 0.7 times the ship's draught as it approximates the average depth of significant noise sources, such as the propeller and machinery [60]. Therefore, the source was modeled at a depth of 4.9 m and located close to the median water depth turbine modeling site of Med Wind A2 (A2-M), remaining adjacent to the tower throughout the servicing time. Siem Sapphire's spectral source levels were then propagated using the propagation environment of the Sicily study area to estimate received levels.

To represent the worst-case scenario, we used the same February sound speed profile considered for modeling the median-depth location of Med Wind A2. The obtained vessel sound field was then added to the aggregate sound of the whole Med Wind farm.

3. Results

3.1. Modeled Propagated Sound and Variations in Relation to the Seasonal Conditions

From propagation modeling, the aggregate sound levels (L_p) for each of the three offshore wind farms and the sound levels (L_p) for the Med Wind OWF plus the support ship in dynamic positioning within the farm were obtained. The sound exposure levels over 24 h are reported in the Supplementary Materials (Table S13).

Table 3 reports the ranges at which given aggregate sound levels are reached for broadband levels (provided every 5 dB). These levels are mapped in Figure 2 (Hannibal and Sicily South in February and August conditions), Figure 3 (detail of the modeled radiated sound field from Hannibal, with February sound speed profile), and Figure 4 (Med Wind in February and August conditions). The distances and contours shown represent the maximum range at which a given sound level is received at any depth in the water column.

The modeling results show that broadband-propagated levels generally decay quickly with distance; within a 1 km radius of the Hannibal wind farm, the sound pressure level goes from 160 to 116 dB re 1 μPa (February SSP). Within the same range, in the case of Sicily South, the level similarly decays from 156 to 112 dB re 1 μPa, and for Med Wind, from 158 to 114 dB re 1 μPa within a 1 km range. In all cases, ranges are longer in February than in August.

Tables 4 and 5 report the levels for the 63 Hz and 125 Hz one-third-octave bands (bands of interest for the MSFD), while Tables 6 and 7 report levels for the 100 Hz and 200 Hz one-third-octave bands, respectively (dominant frequencies' bands).
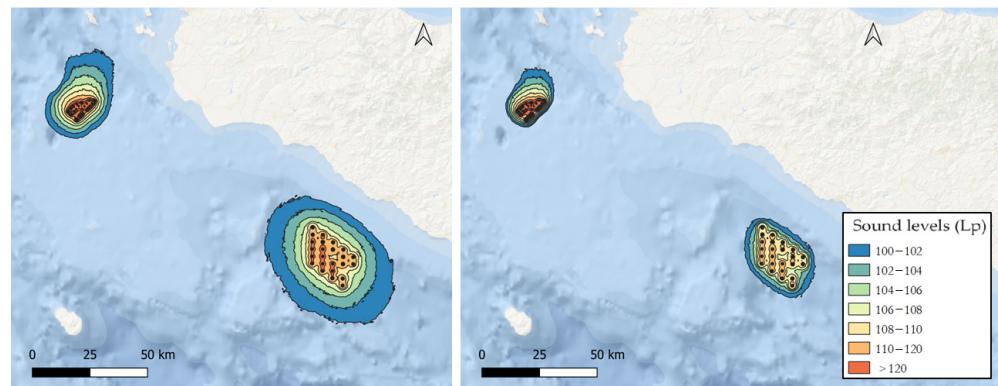
Figure 2. Modeled radiated sound fields (L$_p$) from Hannibal and Sicily South. February sound speed profile was applied to obtain the image on the left, and August was applied on the right. In color scale, sound levels (L$_p$) are represented from 100 dB up to the maximum per wind farm, as reported in the legend.
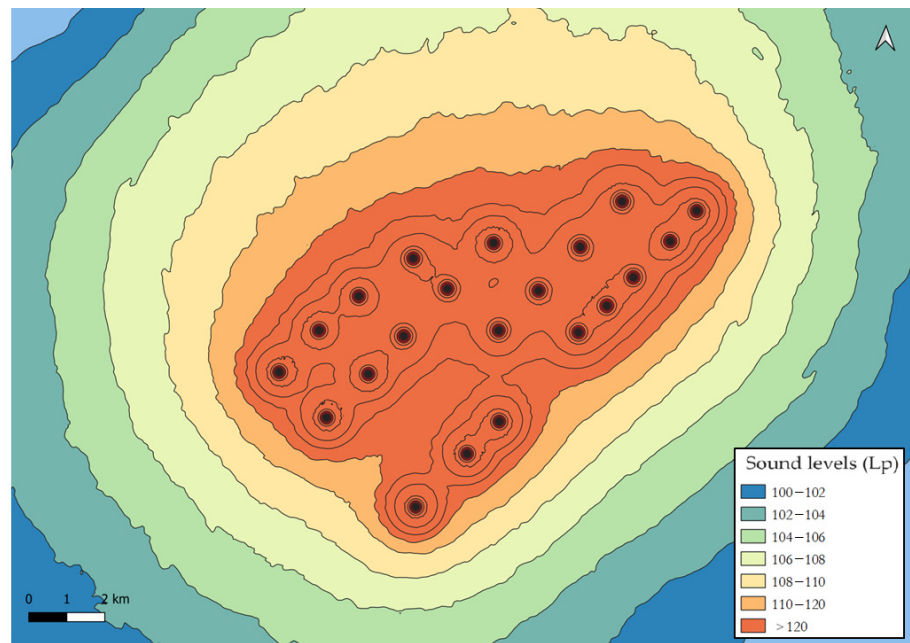
Figure 3. Zoomed modeled radiated sound fields (L$_p$) from Hannibal, with February sound speed profile.
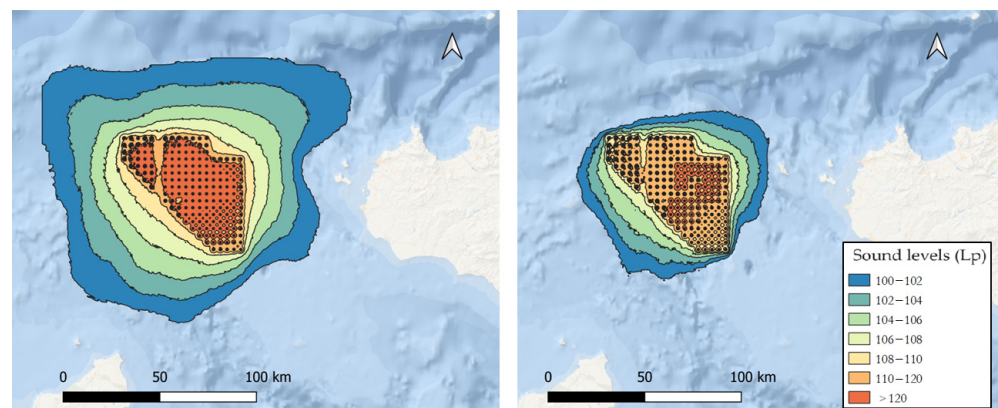
Figure 4. Modeled radiated sound field (L$_p$) from Med Wind. February sound speed profile on the left; August sound speed profile on the right.

Table 3. Hannibal, Sicily South, and Med Wind broadband aggregate sound levels (95th percentile) and the corresponding maximum ranges (in km) for February and August sound speed profiles.

	Hannibal		Sicily South		Med Wind	
L_p (dB re 1 μPa)	February SSP	August SSP	February SSP	August SSP	February SSP	August SSP
	Range (km)	Range (km)	Range (km)	Range (km)	Range (km)	Range (km)
160	<0.03	<0.03	-	-	-	-
155	<0.03	<0.03	<0.04	<0.04	<0.04	<0.04
150	<0.03	<0.03	<0.04	<0.04	<0.04	<0.04
145	<0.03	<0.03	<0.04	<0.04	<0.04	<0.04
140	<0.03	<0.03	0.04	0.04	0.04	0.04
135	0.03	0.03	0.06	0.06	0.07	0.07
130	0.10	0.10	0.09	0.09	0.09	0.09
125	0.14	0.14	0.16	0.13	0.14	0.14
120	0.26	0.26	0.27	0.24	0.25	0.25
115	1.19	1.16	0.54	0.43	0.85	0.79
110	3.74	3.07	3.00	1.90	4.46	3.93
105	9.71	7.19	7.06	3.85	28.66	14.17
100	22.52	15.14	21.59	8.42	67.99	35.67

Table 4. Hannibal, Sicily South, and Med Wind 63 Hz one-third-octave band aggregate sound levels (95th percentile) and the corresponding maximum ranges (in km) for February and August sound speed profiles.

	Hannibal		Sicily South		Med Wind	
L_p (dB re 1 μPa)	February SSP	August SSP	February SSP	August SSP	February SSP	August SSP
	Range (km)	Range (km)	Range (km)	Range (km)	Range (km)	Range (km)
147	<0.03	<0.03	-	-	-	-
145	<0.03	<0.03	-	-	<0.04	<0.04
140	<0.03	<0.03	<0.04	<0.04	<0.04	<0.04
135	<0.03	<0.03	<0.04	<0.04	<0.04	<0.04
130	<0.03	<0.03	0.04	<0.04	0.04	0.04
125	0.03	0.03	0.06	0.04	0.06	0.06
120	0.07	0.07	0.08	0.07	0.08	0.08
115	0.10	0.10	0.13	0.11	0.12	0.12
110	0.21	0.21	0.22	0.18	0.21	0.21
105	0.65	0.60	0.39	0.33	0.53	0.52
100	1.43	1.27	1.10	0.59	2.48	1.08

Table 5. Hannibal, Sicily South, and Med Wind 125 Hz one-third-octave band aggregate sound levels (95th percentile) and the corresponding maximum ranges (in km) for February and August sound speed profiles.

	Hannibal		Sicily South		Med Wind	
L_p (dB re 1 μPa)	February SSP	August SSP	February SSP	August SSP	February SSP	August SSP
	Range (km)	Range (km)	Range (km)	Range (km)	Range (km)	Range (km)
145	<0.03	<0.03	-	-	<0.04	<0.04
140	<0.03	<0.03	<0.04	<0.04	<0.04	<0.04
135	<0.03	<0.03	<0.04	<0.04	0.04	0.04
130	<0.03	<0.03	0.04	0.04	0.06	0.06
125	0.03	0.03	0.06	0.06	0.07	0.07
120	0.08	0.08	0.09	0.08	0.09	0.09
115	0.14	0.14	0.13	0.13	0.14	0.14

Table 5. *Cont.*

Lp (dB re 1 μPa)	Hannibal		Sicily South		Med Wind	
	February SSP	August SSP	February SSP	August SSP	February SSP	August SSP
	Range (km)	Range (km)	Range (km)	Range (km)	Range (km)	Range (km)
110	0.27	0.26	0.22	0.22	0.26	0.24
105	1.16	1.10	0.42	0.40	0.77	0.67
100	3.97	2.63	1.83	1.68	3.95	3.79

Table 6. Hannibal, Sicily South, and Med Wind 100 Hz one-third-octave band aggregate sound levels (95th percentile) and the corresponding maximum ranges (in km) for February and August sound speed profiles.

Lp (dB re 1 μPa)	Hannibal		Sicily South		Med Wind	
	February SSP	August SSP	February SSP	August SSP	February SSP	August SSP
	Range (km)	Range (km)	Range (km)	Range (km)	Range (km)	Range (km)
155	<0.03	< 0.03	<0.04	<0.04	-	-
150	<0.03	<0.03	<0.04	<0.04	<0.04	<0.04
145	<0.03	<0.03	<0.04	<0.04	<0.04	<0.04
140	<0.03	<0.03	<0.04	<0.04	0.04	0.04
135	0.03	0.03	0.04	0.04	0.05	0.05
130	0.07	0.07	0.06	0.06	0.07	0.07
125	0.10	0.10	0.09	0.09	0.11	0.11
120	0.17	0.17	0.16	0.16	0.17	0.16
115	0.54	0.52	0.29	0.27	0.36	0.36
110	1.48	1.27	0.54	0.51	1.72	0.95
105	5.68	3.46	2.74	2.10	8.78	4.22
100	13.46	8.72	6.30	4.24	32.62	21.72

Table 7. Hannibal, Sicily South, and Med Wind 200 Hz one-third-octave band aggregate sound levels (95th percentile) and the corresponding maximum ranges (in km) for February and August sound speed profiles.

| Lp (dB re 1 μPa) | Hannibal | | Sicily South | | Med Wind | |
	February SSP	August SSP	February SSP	August SSP	February SSP	August SSP
	Range (km)	Range (km)	Range (km)	Range (km)	Range (km)	Range (km)
150	<0.03	<0.03	-	-	<0.04	<0.04
145	<0.03	<0.03	<0.04	<0.04	<0.04	<0.04
140	<0.03	<0.03	<0.04	<0.04	<0.04	<0.04
135	<0.03	<0.03	0.04	<0.04	0.04	0.04
130	0.03	0.03	0.06	0.04	0.06	0.06
125	0.07	0.07	0.08	0.07	0.08	0.08
120	0.10	0.10	0.13	0.11	0.12	0.12
115	0.20	0.19	0.22	0.18	0.20	0.19
110	0.99	0.98	0.41	0.33	0.46	0.41
105	3.36	2.67	2.24	0.67	3.95	2.52
100	9.96	6.76	7.18	3.33	28.76	8.91

3.2. Acoustic Contribution of a Maintenance Ship to Operating Med Wind

In Table 8, the ranges at which given broadband aggregate sound levels are reached for the Med Wind OWF, with the addition of the Siem Sapphire support vessel, for February conditions are provided. When the sound of an offshore supply ship is added to the aggregate sound of Med Wind, the radiated sound level increases to 190 dB re 1 μPa within 10 m from the source.

Table 8. Med Wind with offshore support ship broadband aggregate sound levels (95th percentile) and the corresponding maximum ranges (in km) for February sound speed profile.

L_p (dB re 1 μPa)	Range (km)
190	<0.01
165	0.01
160	0.06
155	0.10
150	0.18
145	0.34
140	0.63
135	1.66
130	2.49
125	3.98
120	12.5
115	25.0
110	73.4
105	109
100	131

Figure 5 shows the mapped levels; as before, the distances and contours represent the maximum range at which a given sound level is received at any depth in the water column.
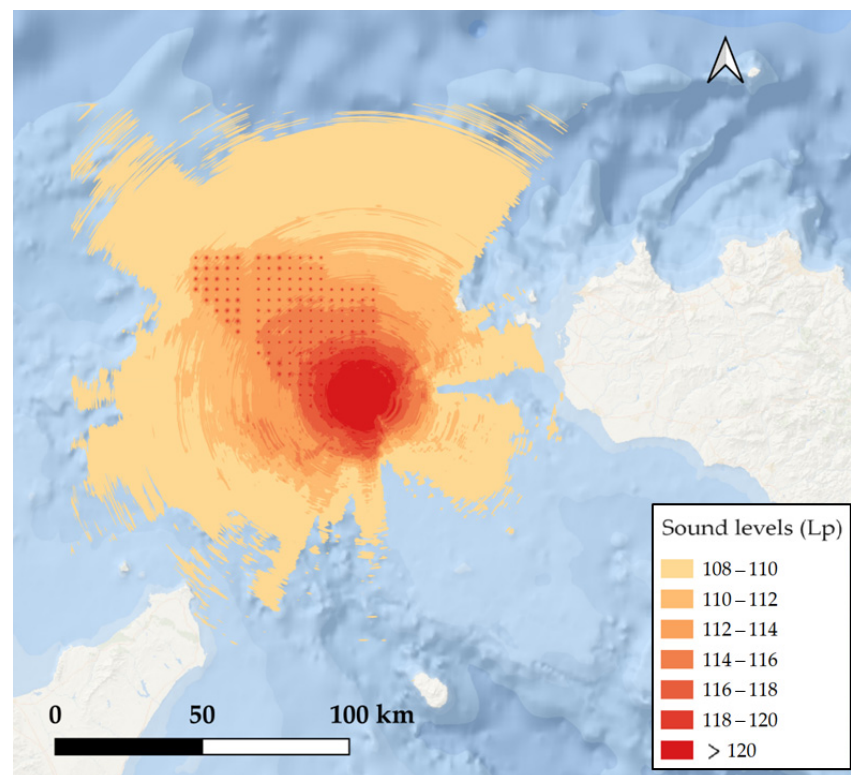
Figure 5. Modeled radiated sound field (L_p) from operational Med Wind plus a support ship on dynamic positioning.

4. Discussion

This work presents the first modeling of the propagated operational sound of three floating offshore wind farms currently planned for construction in the Strait of Sicily. They differ in the number of turbines, bathymetry, and sediment properties. The radiated sound of an offshore support ship was also added to the aggregate sound of the biggest of the three modeled wind farms.

The relevance of this study lies in the fact that many floating offshore wind farms are planned in the Mediterranean Sea, raising concerns for marine ecosystems, especially for marine protected areas. The underwater soundscape will likely be affected by these infrastructures, and potential environmental impacts need to be investigated.

The results show a generally quick decay with distance at the broadband levels, which is in line with the outcomes previously obtained by Tougaard et al. [16], who modeled individual bottom-fixed-foundation turbines, supporting the evidence that propagated levels strongly decrease with distance whether the turbine towers extend to the seafloor in shallower waters or are floating in deeper waters.

Longer ranges were always found in February compared to August, showing the effect of changes in the sound speed profile, especially due to the water temperature. The February sound speed profile is characterized by colder surface waters and a deeper mixed layer, creating a sound channel that allows for longer acoustic propagation ranges [28]. In contrast, the August profile, with warmer surface waters and a shallower mixed layer, results in less efficient sound propagation [28]. This seasonal variation causes sound to travel farther in winter than in summer.

When adding the sound of the offshore supply ship, the acoustic contribution of the maintenance ship dominates the sound footprint of the whole wind farm. Propagated broadband sound levels in February reach 137 dB re 1 μPa at a 1 km distance from the ship, compared to 114 dB re 1 μPa without it.

Most of the scientific literature analyzing noise from offshore wind farms refers to individual fixed-foundation turbines. Tougaard et al. [16] reviewed the literature reporting the measurements of operational underwater noise. The estimated broadband (different frequency ranges) sound levels range from 109 to 137 dB re 1 μPa within 40 m from the turbine [16]. The upper level occurs with turbines of similar power to those considered sources for our study. Our modeled aggregate sound levels reach values from 138 to 158 dB re 1 μPa at 40 m from the wind farm. Furthermore, the source level spectra that we applied included transient sounds associated with the mooring system [23].

Broadband background levels (calculated on 0–48 kHz in 5 min recordings) reported for the Med Wind area from February to April 2022 range from about 105 to a maximum of 150 dB re 1 μPa, with a mean value of 115 dB re 1 μPa [61]. Levels ranging from about 105 to 131 dB re 1 μPa were recorded 5 km off the coast of Capo Granitola, Sicily, in February 2015 [62]. However, these ranges can change related to seasonality [63]. With the support ship holding position in the area, Med Wind modeled levels go beyond 105 dB re 1 μPa (minimum reported background level) at about 100 km from the farm. Without the ship, the same level is exceeded around 25 km from the farm for the same seasonal conditions. At the Hannibal wind farm, an L_p of 105 dB re 1 μPa is exceeded within 10 km in February, and 7 km in August; at Sicily South, this occurs at about 6 km in February and 4 km in August. Therefore, considering our modeling results, operational noise can still be measurable above ambient levels at least 4 km away from any of the wind farms. These results also highlight that the number of turbines, which is the largest for Med Wind, followed by Sicily South, and smallest for Hannibal, only partially determines the sound propagation ranges that are also influenced by environmental parameters and bathymetry.

As is evident from the source spectrum that we applied, the sound generated by turbines is predominant in the frequency bands between 63 Hz and 200 Hz. While specific attention has been paid over the years to the 63 Hz and 125 Hz bands, identified by the Marine Strategy Framework Directive (MSFD) as key indicators, limited information is available for the remaining bands within this range. In the 63 Hz one-third-octave band, previously recorded sound levels in the area range from about 96 to 111 dB re 1 μPa (L_p, Med Wind area) [61], from 82 to 97 dB re 1 μPa (L_p, 5th and 95th percentiles, Marettimo Island, [64]), and from 71 to 119 dB re 1 μPa (L_p, Capo Granitola, [34]). Operational noise generated by the three wind farms reaches the maximum background level in this frequency band from 70 to 90 m. In the 125 Hz one-third-octave band, recorded levels range from about 94 to 105 dB re 1 μPa (Med Wind area, [61]), from 80 to 94 dB re 1 μPa

(L_p, 5th and 95th percentiles, Marettimo Island, [64]), and from 66 to 120 dB re 1 μPa (Capo Granitola, [34]). In this case, aggregate wind farm noise reaches the maximum background level in this frequency band from 80 to 90 m. Furthermore, our results clearly demonstrate that levels of 100 dB re 1 μPa can be reached in the 100 Hz and 200 Hz bands at distances ranging from 3 to 32 km from the source, highlighting significant variability related to the characteristics of the wind farm, environmental factors, and seasonal variations.

These low frequency levels depend on the turbine blades' rotation speed and the number of poles [16]. Operational sound in these bands should be regularly monitored to evaluate possible changes in environmental noise, as mandated by the MSFD.

It must be further recognized that the spectra used for this modeling relate to 6 MW turbines, while the proposed nominal power of single turbines for these three wind farms ranges from 12 to 25 MW. As suggested by Tougaard et al. [16], turbine noise is dependent on wind speed, environmental conditions, and turbine size. Therefore, the modeled scenarios in this study represent fewer impacting conditions than the planned reality; they can nonetheless be considered useful lower estimates of what sound levels might be generated.

As a last consideration, we highlight that the acoustic footprint of at least two of the considered wind farms (Med Wind and Hannibal) could overlap at sound levels of biological relevance, potentially enhancing concerns for the possible environmental impacts in the area.

While our study provides valuable insights into the propagated sound levels from floating offshore wind farms, it is important to acknowledge certain methodological limitations. Firstly, the assumption of a point source for sound propagation, although justified based on far-field considerations, may oversimplify the acoustic characteristics of floating turbines. This approach was chosen due to the lack of expected strong directivity patterns and the focus on aggregate far-field sound, similar to the rationale used for vessel noise modeling. However, it is possible that this approximation might not fully capture the complexities of near-field interactions, particularly in the unique context of floating turbines with larger capacities. Additionally, the placement of the point source at the midpoint of the submerged section, while consistent with previous studies, may not entirely represent the acoustic behavior of the submerged structure, which could act more as an array source. These considerations suggest that while our model provides a reasonable estimate for far-field sound propagation, further research is needed to refine these assumptions, particularly in light of the evolving turbine designs and capacities. Finally, our study highlights the need for future empirical investigations into the influence of turbine capacity and geometry and environmental factors on sound propagation, as these variables are likely to play critical roles that our current methodology could not fully address.

Modeling can provide valuable insights into the optimal layout and number of turbines needed to minimize potential environmental impacts. By modeling the combined effects of multiple wind farms, it is possible to assess cumulative impacts and determine whether the sound footprint remains localized or escalates when wind farms are situated near each other. These findings could also help establish minimum distance requirements between wind farms to mitigate potential adverse effects. Based on the results of this study, it may be advisable to conduct sound recordings at fixed intervals throughout the operational phase under varying conditions to evaluate any increase in sound levels generated by the wind farms. A systematic monitoring protocol should be established, involving measurements at predetermined distances from the turbines and at specified depths, to ensure the consistency and comparability of the data over time. Furthermore, it could be useful to develop a comprehensive database that includes data from a range of turbines, mooring systems, and operational conditions. This database should also contain detailed information on turbine specifications, such as rotational speed (RPM), number of poles, gearbox versus direct drive systems, and the ability to integrate this information with field data on weather conditions. This approach will enable the accumulation of standardized data that can be used for longitudinal studies and comparative analyses across different sites and technologies.

References

1. Global Wind Energy Council. Global Wind Report 2024. Available online: www.gwec.net (accessed on 20 June 2024).
2. Farr, H.; Ruttenberg, B.; Walter, R.K.; Wang, Y.H.; White, C. Potential environmental effects of deepwater floating offshore wind energy facilities. *Ocean Coast. Manag.* **2021**, *207*, 105611. [CrossRef]
3. Galparsoro, I.; Menchaca, I.; Garmendia, J.M.; Borja, Á.; Maldonado, A.D.; Iglesias, G.; Bald, J. Reviewing the ecological impacts of offshore wind farms. *Npj Ocean Sustain.* **2022**, *1*, 1–8. [CrossRef]
4. Lloret, J.; Turiel, A.; Solé, J.; Berdalet, E.; Sabatés, A.; Olivares, A.; Gili, J.M.; Vila-Subirós, J.; Sardá, R. Unravelling the ecological impacts of large-scale offshore wind farms in the Mediterranean Sea. *Sci. Total Environ.* **2022**, *824*, 153803. [CrossRef] [PubMed]
5. Rezaei, F.; Contestabile, P.; Vicinanza, D.; Azzellino, A. Towards understanding environmental and cumulative impacts of floating wind farms: Lessons learned from the fixed-bottom offshore wind farms. *Ocean Coast. Manag.* **2023**, *243*, 106772. [CrossRef]
6. Watson, S.C.L.; Somerfield, P.J.; Lemasson, A.J.; Knights, A.M.; Edwards-Jones, A.; Nunes, J.; Pascoe, C.; McNeill, C.L.; Schratzberger, M.; Thompson, M.S.A.; et al. The global impact of offshore wind farms on ecosystem services. *Ocean Coast. Manag.* **2024**, *249*, 107023. [CrossRef]
7. Lloret, J.; Wawrzynkowski, P.; Dominguez-Carrió, C.; Sardá, R.; Molins, C.; Gili, J.M.; Sabatés, A.; Vila-Subirós, J.; Garcia, L.; Solé, J.; et al. Floating offshore wind farms in Mediterranean marine protected areas: A cautionary tale. *ICES J. Mar. Sci.* **2023**, fsad131. [CrossRef]
8. Carroll, A.G.; Przeslawski, R.; Duncan, A.; Gunning, M.; Bruce, B. A critical review of the potential impacts of marine seismic surveys on fish & invertebrates. *Mar. Pollut. Bull.* **2017**, *114*, 9–24. [CrossRef]
9. Duarte, C.M.; Chapuis, L.; Collin, S.P.; Costa, D.P.; Devassy, R.P.; Eguiluz, V.M.; Erbe, C.; Gordon, T.A.C.; Halpern, B.S.; Harding, H.R.; et al. The soundscape of the Anthropocene ocean. *Science* **2021**, *371*, 6529. [CrossRef]
10. Hildebrand, J.A. Anthropogenic and natural sources of ambient noise in the ocean. *Mar. Ecol. Prog. Ser.* **2009**, *395*, 5–20. [CrossRef]
11. Popper, A.N.; Hawkins, A. *The Effects of Noise on Aquatic Life II*; Springer: New York, NY, USA, 2016. Available online: http://www.springer.com/series/5584 (accessed on 20 June 2024).
12. European Parliament and Council. Directive 2008/2056/EC of the European Parliament and of the Council of 17 June 2008 Establishing a Framework for Community Action in the Field of Marine Environmental Policy (Marine Strategy Framework Directive) (Brussels, Belgium). Available online: https://eur-lex.europa.eu/legal-content/EN/TXT/?uri=CELEX:32008L0056 (accessed on 20 June 2024).

13. European Parliament and Council. Commission Decision (EU) 2017/848 of 17 May 2017 Laying Down Criteria and Methodological Standards on Good Environmental Status of Marine Waters and Specifications and Standardised Methods for Monitoring and Assessment, and Repealing Decision 2010/477/EU. Available online: https://eur-lex.europa.eu/eli/dec/2017/848/oj (accessed on 20 June 2024).

14. Elliott, J.; Khan, A.A.; Lin, Y.-T.; Mason, T.; Miller, J.H.; Newhall, A.E.; Potty, G.R.; Vigness-Raposa, K.J. Field Observations During Wind Turbine Operations at the Block Island Wind Farm, Rhode Island. Final Report to the U.S. Department of the Interior, Bureau of Ocean Energy Management, Office of Renewable Energy Programs, OCS Study BOEM 2019-028. 2019; p. 281. Available online: https://espis.boem.gov/final%20reports/BOEM_2019-028.pdf (accessed on 20 June 2024).

15. Pangerc, T.; Theobald, P.D.; Wang, L.S.; Robinson, S.P.; Lepper, P.A. Measurement and characterisation of radiated underwater sound from a 3.6 MW monopile wind turbine. *J. Acoust. Soc. Am.* **2016**, *140*, 2913–2922. [CrossRef]

16. Tougaard, J.; Hermannsen, L.; Madsen, P.T. How loud is the underwater noise from operating offshore wind turbines? *J. Acoust. Soc. Am.* **2020**, *148*, 2885–2893. [CrossRef] [PubMed]

17. Yoon, Y.G.; Han, D.G.; Choi, J.W. Measurements of underwater operational noise caused by offshore wind turbine off the southwest coast of Korea. *Front. Mar. Sci.* **2023**, *10*, 1153843. [CrossRef]

18. Barooni, M.; Ashuri, T.; Velioglu Sogut, D.; Wood, S.; Ghaderpour Taleghani, S. Floating Offshore Wind Turbines: Current Status and Future Prospects. *Energies* **2023**, *16*, 2. [CrossRef]

19. Chen, J.; Kim, M.-H. Review of Recent Offshore Wind Turbine Research and Optimization Methodologies in Their Design. *J. Mar. Sci. Eng.* **2022**, *10*, 28. [CrossRef]

20. Betke, K.; Schultz-Von Glahn, M.; Matuschek, R. Underwater Noise Emissions from Offshore Wind Turbines. Proc CFA/DAGA 2004. Strasbourg. Available online: https://tethys.pnnl.gov/sites/default/files/publications/Betke-2004.pdf (accessed on 20 June 2024).

21. Madsen, P.; Wahlberg, M.; Tougaard, J.; Lucke, K.; Tyack, P. Wind turbine underwater noise and marine mammals: Implications of current knowledge and data needs. *Mar. Ecol. Prog. Ser.* **2006**, *309*, 279–295. [CrossRef]

22. Sigray, P.; Andersson, M.H. Particle motion measured at an operational wind turbine in relation to hearing sensitivity in fish. *J. Acoust. Soc. Am.* **2011**, *130*, 200–207. [CrossRef]

23. Pace, F.; Burns, R.D.J.; Martin, S.B.; Wood, M.A.; Wilson, C.C.; Lumsden, C.E.; Murvoll, K.M.; Weissenberger, J. Underwater Sound Emissions from the Moorings of Floating Wind Turbines: HYWIND Scotland Case Study. In *The Effects of Noise on Aquatic Life*; Springer Nature: Cham, Switzerland, 2024; pp. 1–23. [CrossRef]

24. Risch, D.; Favill, G.; Marmo, B.; Van Geel, N.; Benjamins, S.; Thompson, P.; Wittich, A.; Wilson, B. Characterisation of UNDER-WATER Operational Noise of Two Types of Floating Offshore Wind Turbines. Executive Summary. 2023. Available online: https://tethys.pnnl.gov/sites/default/files/publications/Rischetal.pdf (accessed on 20 June 2024).

25. Burns, R.D.J.; Martin, S.B.; Wood, M.A.; Wilson, C.C.; Lumsden, C.E.; Pace, F. *Hywind Scotland Floating Offshore Wind Farm. Sound Source Characterisation of Operational Floating Turbines*; Document 02521, Version 3.0 FINAL; Technical Report by JASCO Applied Sciences (UK) Ltd. for Equinor Energy AS: Stavanger, Norway, 2022.

26. Thomsen, F.; Stöber, U.; Sarnocińska-Kot, J. Hearing Impact on Marine Mammals Due to Underwater Sound from Future Wind Farms. In *The Effects of Noise on Aquatic Life*; Springer Nature: Cham, Switzerland, 2023. [CrossRef]

27. Etter, P.C. *Underwater Acoustic Modeling and Simulation*, 4th ed.; CRC Press: Boca Raton, FL, USA, 2013. [CrossRef]

28. Jensen, F.; Kuperman, W.; Porter, M.; Schmidt, H. *Computational Ocean Acoustics, 2nd ed*; Springer: New York, NY, USA, 2011. [CrossRef]

29. Urick, R.J. *Principles of Underwater Sound*, 3rd ed.; McGraw-Hill: New York, NY, USA, 1983.

30. Stöber, U.; Thomsen, F. How could operational underwater sound from future offshore wind turbines impact marine life? *J. Acoust. Soc. Am.* **2021**, *149*, 1791–1795. [CrossRef]

31. 4C Offshore. Available online: https://www.4coffshore.com/windfarms/italy/ (accessed on 17 June 2024).

32. Di Lorenzo, M.; Sinerchia, M.; Colloca, F. The North sector of the Strait of Sicily: A priority area for conservation in the Mediterranean Sea. *Hydrobiologia* **2018**, *821*, 235–253. [CrossRef]

33. Maggio, T.; Perzia, P.; Pazzini, A.; Campagnuolo, S.; Falautano, M.; Mannino, A.M.; Allegra, A.; Castriota, L. Sneaking into a Hotspot of Biodiversity: Coverage and Integrity of a Rhodolith Bed in the Strait of Sicily (Central Mediterranean Sea). *J. Mar. Sci. Eng.* **2022**, *10*, 1808. [CrossRef]

34. Papale, E.; Alonge, G.; Grammauta, R.; Ceraulo, M.; Giacoma, C.; Mazzola, S.; Buscaino, G. Year-round acoustic patterns of dolphins and interaction with anthropogenic activities in the Sicily Strait, central Mediterranean Sea. *Ocean. Coast. Manag.* **2020**, *197*, 105320. [CrossRef]

35. Erbe, C.; Marley, S.A.; Schoeman, R.P.; Smith, J.N.; Trigg, L.E.; Embling, C.B. The Effects of Ship Noise on Marine Mammals—A Review. *Front. Mar. Sci.* **2019**, *6*, 606. [CrossRef]

36. Maglio, A.; Pavan, G.; Castellote, M.; Frey, S. Overview of the Noise Hot Spots in the ACCOBAMS Area—Part I, Mediterranean Sea. ACCOBAMS-MOP6/2016/Doc28Rev1. 2016. Available online: https://accobams.org/wp-content/uploads/2020/01/MOP6.Doc28Rev1_Overview_noise_hot_spots_-ACCOBAMS_area_Part_Mediterranean.pdf (accessed on 20 August 2024).

37. 7SeasMed. Dott. Ing. Luigi Severini. Progetto per la Realizzazione di un Parco Eolico Offshore di Tipo Floating nel Canale di Sicilia. Studio di Impatto Ambientale. 2021. Available online: https://va.mite.gov.it/it-IT/Oggetti/Documentazione/7273/10503 (accessed on 20 June 2024).

38. AvenHexicon. Progetto di una Centrale Eolica Offshore Galleggiante nel Canale di Sicilia Denominata "Sicily South" e delle Relative Opere di Connessione Alla Rete Elettrica Nazionale. Studio Preliminare Ambientale. 2023. Available online: https://va.mite.gov.it/it-IT/Oggetti/Documentazione/9331/13691 (accessed on 20 June 2024).

39. Renexia S.p.A. Progetto di una Centrale Eolica Offshore Galleggiante nel Canale di Sicilia e delle Relative Opere di Connessione alla Rete Elettrica Nazionale. Studio Preliminare Ambientale. 2020. Available online: https://va.mite.gov.it/en-GB/Oggetti/Info/7634 (accessed on 20 June 2024).

40. GEBCO—The General Bathymetric Chart of the Oceans. 2023. Available online: https://download.gebco.net/ (accessed on 20 June 2024).

41. European Marine Observation and Data Network. 2023. Available online: https://emodnet.ec.europa.eu/geoviewer/ (accessed on 20 June 2024).

42. Roddier, D.; Cermelli, C.; Aubault, A.; Weinstein, A. WindFloat: A floating foundation for offshore wind turbines. *J. Renew. Sustain. Energy* **2010**, *2*, 033104. [CrossRef]

43. Copernicus Marine Service. Global Ocean Daily Gridded Reprocessed L3 Sea Surface Winds from Scatterometer. Available online: https://data.marine.copernicus.eu/product/WIND_GLO_PHY_L3_MY_012_005/description (accessed on 20 June 2024).

44. MacGillivray, A.O.; Chapman, R.N. Modeling Underwater Sound Propagation from an Airgun Array Using the Parabolic Equation Method. *Spec. Mar. Acoust.* **2012**, *40*, 19–25. Available online: https://jcaa.caa-aca.ca/index.php/jcaa/article/view/2502 (accessed on 20 June 2024). [CrossRef]

45. Collins, M.D. A split-step Padé solution for the parabolic equation method. *J. Acoust. Soc. Am.* **1993**, *93*, 1736–1742. [CrossRef]

46. Porter, M.B.; Liu, Y.C. Finite-element ray tracing. In *International Conference on Theoretical and Computational Acoustics*; Lee, D., Schultz, M.H., Eds.; World Scientific Publishing Co.: Hackensack, NJ, USA, 1994; Volume 2, pp. 947–956.

47. Aerts, L.A.M.; Blees, M.; Blackwell, S.B.; Greene, C.R., Jr.; Kim, K.H.; Hannay, D.E.; Austin, M.E. *Marine Mammal Monitoring and Mitigation during BPXA Liberty OBC Seismic Survey in Foggy Island Bay, Beaufort Sea, July–August 2008: 90-Day Report*; LGL Report P1011-1; LGL Ltd.: Bryan, TX, USA; Alaska Research Associates, Inc.: Anchorage, AK, USA; Greeneridge Sciences, Inc.: Goleta, CA, USA; JASCO Applied Sciences (formerly JASCO Research Ltd.): Victoria, BC, Canada, 2008; 199p.

48. Funk, D.W.; Hannay, D.E.; Ireland, D.S.; Rodrigues, R.; Koski, W.R. *Marine Mammal Monitoring and Mitigation during Open Water Seismic Exploration by Shell Offshore Inc. in the Chukchi and Beaufort Seas, July–November 2007: 90-Day Report*; LGL Report P969-1; LGL Ltd.: Bryan, TX, USA; Alaska Research Associates, Inc.: Anchorage, AK, USA; JASCO Applied Sciences (formerly JASCO Research Ltd.): Victoria, BC, Canada; Shell Offshore Inc.: Houston, TX, USA; National Marine Fisheries Service: Silver Spring, MD, USA; US Fish and Wildlife Service: Washington, DC, USA, 2008; 218p.

49. Hannay, D.E.; Racca, R. *Acoustic Model Validation*; Technical Report 0000-S-90-04-T-7006-00-E, Rev. 02, V. 1.3; JASCO Applied Sciences (formerly JASCO Research Ltd.): Victoria, BC, Canada; Sakhalin Energy Investment Company, Ltd.: Yuzhno-Sakhalinsk, Russia, 2005; 34p.

50. Ireland, D.S.; Rodrigues, R.; Funk, D.W.; Koski, W.R.; Hannay, D.E. *Marine Mammal Monitoring and Mitigation during Open Water Seismic Exploration by Shell Offshore Inc. in the Chukchi and Beaufort Seas, July–October 2008: 90-Day Report*; LGL Report P1049-1; LGL Ltd.: Bryan, TX, USA; Alaska Research Associates, Inc.: Anchorage, AK, USA, 2009; 277p.

51. Martin, S.B.; Bröker, K.; Matthews, M.-N.R.; MacDonnell, J.T.; Bailey, L. Comparison of measured and modeled air-gun array sound levels in Baffin Bay, West Greenland. In Proceedings of the OceanNoise 2015, Barcelona, Spain, 11–15 May 2015.

52. O'Neill, C.; Leary, D.; McCrodan, A. Sound Source Verification (Chapter 3). In *Marine Mammal Monitoring and Mitigation During Open Water Seismic Exploration by Statoil USA E&P Inc. in the Chukchi Sea, August-October 2010: 90-Day Report*; Blees, M.K., Hartin, K.G., Ireland, D.S., Hannay, D.E., Eds.; LGL Report P1119; LGL Ltd.: Bryan, TX, USA; Alaska Research Associates, Inc.: Anchorage, AK, USA; JASCO Applied Sciences (formerly JASCO Research Ltd.): Victoria, BC, Canada; Statoil USA E&P, Inc.: Houston, TX, USA; National Marine Fisheries Service: Silver Spring, MD, USA; US Fish and Wildlife Service: Washington, DC, USA, 2010; pp. 1–34.

53. Racca, R.; Rutenko, A.N.; Bröker, K.; Austin, M.E. A line in the water—Design and enactment of a closed loop, model based sound level boundary estimation strategy for mitigation of behavioural impacts from a seismic survey. In Proceedings of the 11th European Conference on Underwater Acoustics, Edinburgh, UK, 2–6 July 2012; Volume 34.

54. Racca, R.; Rutenko, A.N.; Bröker, K.; Gailey, G. Model Based Sound Level Estimation and in-Field Adjustment for Real-Time Mitigation of Behavioural Impacts From a Seismic Survey and Post-Event Evaluation of Sound Exposure for Individual Whales. In Proceedings of the Acoustics 2012, Fremantle, Australia, 21–23 November 2012; McMinn, T., Ed. Available online: http://www.acoustics.asn.au/conference_proceedings/AAS2012/papers/p92.pdf (accessed on 20 June 2024).

55. Warner, G.A.; Erbe, C.; Hannay, D.E. Underwater Sound Measurements. In *Marine Mammal Monitoring and Mitigation during Open Water Shallow Hazards and Site Clearance Surveys by Shell Offshore Inc. in the Alaskan Chukchi Sea, July-October 2009: 90-Day Report*; Reiser, C.M., Funk, D., Rodrigues, R., Hannay, D.E., Eds.; LGL Report P1112-1; LGL Ltd.: Bryan, TX, USA; Alaska Research Associates, Inc.: Anchorage, AK, USA; JASCO Applied Sciences (formerly JASCO Research Ltd.): Victoria, BC, Canada; Shell Offshore, Inc.: Houston, TX, USA; National Marine Fisheries Service: Silver Spring, MD, USA; US Fish and Wildlife Service: Washington, DC, USA, 2009; Chapter 3, pp. 1–54.

56. Carnes, M.R. Description and Evaluation of GDEM-V 3.0. US Naval Research Laboratory, Stennis Space Center, MS. NRL Memorandum Report 7330-09-9165; 21p. Available online: https://www.researchgate.net/publication/235013345_Description_and_Evaluation_of_GDEM-V_30 (accessed on 20 June 2024).

57. Teague, W.J.; Carron, M.J.; Hogan, P.J. A Comparison Between the Generalized Digital Environmental Model and Levitus climatologies. *J. Geophys. Res. Oceans* **1990**, *95*, 7167–7183. [CrossRef]

58. Hamilton, E.L. Geoacoustic modeling of the sea floor. *J. Acoust. Soc. Am.* **1980**, *68*, 1313–1340. [CrossRef]

59. McPherson, C.R.; Li, Z.; Wilson, C.C.; Kowarski, K.A.; Koessler, M.W. Beach Otway Development Acoustic Monitoring: Characterisation, Validation, and Marine Mammals. Document 02424, Version 2.0. Technical Report by JASCO Applied Sciences for Beach Energy Limited. 2021. Available online: https://docs.nopsema.gov.au/A802937#page=418 (accessed on 20 June 2024).

60. Sakai, M.; Haga, R.; Tsuchiya, T.; Akamatsu, T.; Umeda, N. Statistical analysis of measured underwater radiated noise from merchant ships using ship operational and design parameters. *J. Acoust. Soc. Am.* **2023**, *154*, 1095–1105. [CrossRef]

61. Sorrentino, G. Bottom Trawling: Characterization of Acoustic Noise and Interaction with Cetaceans in the Central Mediterranean Sea. Master's Thesis, Università degli Studi di Napoli "Federico II", Napoli, Italy, 2023.

62. Papale, E.; (National Recearch Council, Rome, Italy). Personal communication, 2024.

63. Ceraulo, M.; Papale, E.; Caruso, F.; Filiciotto, F.; Grammauta, R.; Parisi, I.; Mazzola, S.; Farina, A.; Buscaino, G. Acoustic comparison of a patchy Mediterranean shallow water seascape: Posidonia oceanica meadow and sandy bottom habitats. *Ecol. Indic.* **2018**, *85*, 1030–1043. [CrossRef]

64. Buscaino, G.; Filiciotto, F.; Fossati, C.; Grammauta, R.; Mazzola, S.; Papale, E.; Pavan, G. Programmi di Monitoraggio "Strategia Marina". In *Attuazione Dell'art*; 11 del D.lgs. 190/2010 ed Elaborati ai Sensi del D.M. 11 Febbraio 2015. Programma 7, Rumore Sottomarino. Technical Report; Ministero dell'Ambiente e della Sicurezza Energetica: Rome, Italy, 2017.